

Complex Patterns in a Simple System

John E. Pearson
Center for Nonlinear Studies
Los Alamos National Laboratory

November 26, 2024

Abstract

Numerical simulations of a simple reaction–diffusion model reveal a surprising variety of irregular spatio–temporal patterns. These patterns arise in response to finite–amplitude perturbations. Some of them resemble the steady irregular patterns discussed by Lee et al. in this issue of *Science* [1]. Others consist of spots which grow until they reach a critical size at which time they divide in two. If, in some region, the spots become over–crowded, all the spots in that region decay into the uniform background.

Patterns occur in nature at scales ranging from the developing *Drosophila* embryo to the large-scale structure of the universe. At the familiar mundane scales we see snowflakes, cloud streets, and sand ripples. We see convective roll patterns in hydrodynamic experiments. We see regular and almost regular patterns in the concentrations of chemically reacting and diffusing systems. As a consequence of the enormous range of scales over which pattern formation occurs, the discovery of any new pattern formation phenomenon is potentially of great scientific interest. In this article, I describe patterns recently observed in numerical experiments on a simple reaction-diffusion model. These patterns are unlike any that have been previously observed in theoretical or numerical studies.

The system is a variant of the autocatalytic Selkov model of glycolysis [2] and is due to Gray and Scott [3]. A variety of spatio-temporal patterns form in response to finite-amplitude perturbations. The response of this model to such perturbations was previously studied in one space dimension by Vastano et al. who showed that steady spatial patterns could form even when the diffusion coefficients were equal [4]. The response of the system in one space dimension is nontrivial and depends both on the control parameters and on the initial perturbation. It will be shown that the patterns that occur in two dimensions range from the well-known regular hexagons to irregular steady patterns similar to those recently observed by Lee et al. [1], to chaotic spatio-temporal patterns. For the ratio of diffusion coefficients used, there are no stable Turing patterns.

Most work in this field in the past has focused on pattern formation from a spatially uniform state that is near the transition from linear stability to linear instability. With this restriction, standard bifurcation-theoretic tools such as amplitude equations have been developed and used with considerable success [5]–[6]. It is unclear whether the patterns presented in this article will yield to these now-standard technologies.

The Gray-Scott model corresponds to the following two reactions:



Both reactions are irreversible so P is an inert product. A nonequilibrium constraint is represented by a feed term for U . Both U and V are removed by

the feed process. The resulting reaction–diffusion equations in dimensionless units are

$$\begin{aligned}\frac{\partial U}{\partial t} &= D_u \nabla^2 U - UV^2 + F(1 - U) \\ \frac{\partial V}{\partial t} &= D_v \nabla^2 V + UV^2 - (F + k)V \quad ,\end{aligned}\tag{2}$$

where k is the dimensionless rate constant of the second reaction and F is the dimensionless feed rate. The system size is 2.5×2.5 , $D_u = 2 \times 10^{-5}$ and $D_v = 10^{-5}$. The boundary conditions are periodic. Before the numerical results are presented, let us consider the the behavior of the reaction kinetics which are described by the ordinary differential equations that result upon dropping the diffusion terms in Eq. 2.

Figure 1 is a phase diagram. A trivial steady state $U = 1, V = 0$ exists and is linearly stable for all F and k . In the region bounded above by the solid line and below by the dotted line, the system is bistable. For fixed k the nontrivial stable uniform solution loses stability via saddle–node bifurcation as F is increased through the upper solid line or by Hopf bifurcation as F is decreased through the dotted line [7]. In the case at hand the bifurcating periodic solution is stable for $k < .035$ and unstable for $k > .035$. There is no periodic orbit for parameter values outside the region enclosed by the solid line.

The simulations are forward Euler integration of the finite difference equations resulting from discretization of the diffusion operator. The spatial mesh consists of 256×256 grid points. The time step used is 1. Spot checks made with meshes as large as 1024×1024 and time steps as small as .01 produce no qualitative difference in the results.

Initially, the entire system was placed in the trivial state ($U = 1, V = 0$). Then the 20×20 mesh point area located symmetrically about the center of the grid was perturbed to ($U = 1/2, V = 1/4$). These conditions were then perturbed with $\pm 1\%$ random noise in order to break the square symmetry. The system was then integrated for 200,000 time steps and an image saved. In all cases, the initial disturbance propagated outward from the central square until the entire grid was affected by the initial square perturbation. The propagation was wavelike, with the leading edge of the perturbation moving with an approximately constant velocity. Depending on the parameter values, it took on the order of 10,000–20,000 time steps

for the initial perturbation to spread over the entire grid. The propagation velocity of the initial perturbation is thus on the order of 1×10^{-4} space units per time unit. After the initial period during which the perturbation spreads, either the system goes into a time dependent state, or to an essentially steady state.

Figures 2 and 3 are phase diagrams. One can view Figure 3 as a map and Figure 2 as the key to the map. The twelve patterns illustrated in Figure 2 and are designated by Greek letters and will be referred to as “pattern α ”, “pattern β ”, etc. The color indicates the concentration of U with red representing $U = 1$ and blue representing $U \approx .2$. Yellow is intermediate to red and blue. In Figure 3, the Greek characters indicate the type of pattern found at that point in parameter space. There are two additional symbols in Figure 3, “R”’s and “B”’s indicating spatially uniform red and blue states respectively. The red state corresponds to $(U = 1, V = 0)$ and the blue state depends on the exact parameter values but corresponds roughly to $(U = .3, V = .25)$.

Pattern α is time-dependent and consists of fledgling spirals which are constantly colliding and annihilating each other: full spirals never form. Pattern β is time-dependent and consists of what is generally called phase turbulence [9] which occurs in the vicinity of a Hopf bifurcation to a stable periodic orbit. The medium is unable to synchronize so the phase of the oscillators varies as a function of position. In the present case the small amplitude periodic orbit that bifurcates is unstable. Pattern γ is time dependent. It consists primarily of stripes as illustrated but there are small localized regions that oscillate with a relatively high frequency $\approx 10^{-3}$. The active regions disappear but new ones always appear elsewhere. In Figure 2 there is an active region near the top center of pattern γ . Pattern δ consists of regular hexagons except for apparently stable defects.

Pattern η is time dependent: a few of the stripes oscillate without apparent decay, but the remainder of the pattern remains time independent.

Pattern ι is time independent and was observed for only a single parameter value.

Patterns θ , κ , and μ resemble those observed by Lee et al. and described in this issue of *Science* [1]. When blue waves collided, they stopped, as did the waves observed by Lee. In pattern μ , long stripes grew in length. The growth was parallel to the stripes and took place at the tips. If two distinct stripes were both growing and were pointed directly at each other, it was

always observed that when the growing tips reached some critical separation distance, they would alter their course so as not to collide. In patterns θ and κ the perturbations grew radially outward with a velocity that was normal to the stripes. In this case if two stripes collided, they simply stopped, as did those observed by Lee. In simulations in one space dimension, I have also observed fronts propagating towards each other that stop when they reach a critical separation. This is fundamentally new behavior for nonlinear waves.

Patterns ε , ζ , and λ are the most interesting and share similarities. They consist of blue spots on a red or yellow background. Pattern λ is time independent and patterns ε and ζ are time dependent. Note that spots occur only in regions of parameter space where the sole uniform steady state is the red state ($U = 1, V = 0$). Thus, the blue spots cannot exist for extended time unless there is a gradient present. Since the gradient is required for the existence of the spots, they must have a maximum size otherwise there would be blue regions that were essentially gradient free. Such regions would necessarily decay to the red state. Note that these gradients are self-sustaining and *not* imposed externally. After the initial perturbation, the spots increase in number until they fill the system. How do they increase their number? After a spot is formed, it grows. When it achieves the critical size the gradient is no longer sufficient to maintain the center of the spot in the blue state so the center decays to red leaving two blue spots. This process is illustrated in Figure 4. The subsequent evolution depends on the control parameters. Pattern λ remains in a steady state. Pattern ζ remains time dependent but with long-range spatial order except for local regions of activity. The active regions are not stationary. At anyone instant they do not appear significantly different from pattern ζ as illustrated in Figure 2 but the location of the red disturbances changes with time. Pattern ε appears to have no long-range order either in time or space. Once the system is filled with blue spots, they can die due to over-crowding. This occurs when many spots are crowded together and the gradient becomes insufficient to support them. The spots in this extended region will collapse nearly simultaneously leaving an irregular red hole. There are always more spots on the boundary of any hole and after a few thousand time steps no sign of the hole will remain. The spots on its border will have filled it. Figures 4 and 5 illustrate the birth and death of the spots in pattern ε .

Figure 6 provides an estimate of the largest Liapunov exponent for pattern ε . The system (with $F = .02, k = .059$) was evolved for 20,000 time steps.

Then a copy of the system was made and randomly perturbed with noise on the order of 1×10^{-12} . The perturbed state served as the initial condition for the copy which was then evolved simultaneously with the original. This was done 20 times and an average was taken. Figure 6 is a Log_{10} -linear plot of $D(t)$ versus t where

$$D(t) = \langle |d| \rangle$$

and $|d|$ is the space average of the absolute value of the difference between the perturbed solution and the unperturbed solution. The angular brackets indicate that an ensemble average was taken. One can clearly see the straight line positive slope dependence indicating exponential growth of errors—the hallmark of chaos. The Liapunov exponent is on the order of 1.5×10^{-3} . The Liapunov time (the inverse of the Liapunov exponent) is 660 time steps. It is roughly equal to the time it takes for a spot to reproduce as shown in Figure 4. This time is also on the order of the time it takes for a molecule to diffuse across one of the blue spots.

All of the patterns presented here arose in response to finite-amplitude perturbations. The ratio of diffusion coefficients used was 2. It is now well known that Turing instabilities which lead to spontaneous pattern formation cannot occur in systems in which all diffusion coefficients are equal. For a comprehensive discussion of these issues see Pearson [8]-[10]. For a discussion of Turing instabilities in the model at hand, see Vastano et al [11]. The only Turing patterns that can occur bifurcate off the nontrivial steady uniform state (the blue state). With the ratio of diffusion coefficients used here, they occur only in a narrow parameter region in the vicinity of ($F = k = .0625$) where the line of saddle-node bifurcations coalesces with the line of Hopf bifurcations. In the vicinity of this point it was shown that the branch of small amplitude Turing patterns is unstable [11]. The smallest ratio of diffusion coefficients that gives stable Turing patterns is about $D_u/D_v = 2.8$.

No pattern formation occurred when the diffusion coefficients were equal although target patterns were observed. The target patterns consisted of an oscillating core located at the center of the initially perturbed region. The core oscillated, apparently without decay, continually launching waves into the medium. With equal diffusion coefficients, no patterns formed in which the small asymmetries in the initial conditions were amplified by the dynamics. This observation can probably be understood in terms of the following fact. Nonlinear plane waves in two dimensions cannot be destabilized

by diffusion in the case that all diffusion coefficients are equal [12]. During the initial stages of the evolution, the corners of the square perturbation are rounded off. Then the perturbation evolves as a radial wave, either inward or outward depending on the parameter values. Such a wave cannot undergo spontaneous symmetry breaking unless the diffusion coefficients are unequal. However, as demonstrated in the current article, I found symmetry breaking over a wide range of parameter values for a ratio of diffusion coefficients of 2. Such a ratio is physically reasonable even for small molecules in aqueous solution.

The similarity of the Gray–Scott model to the Selkov model of glycolysis may be of biological relevance. Recently Hasslacher et al., have demonstrated the plausibility of sub-cellular chemical patterns via lattice–gas simulations of the Selkov model [13]. The patterns discussed in the present article are likely to be found in the Selkov model as well, and thus it is plausible that they are relevant to glycolysis.

References

- [1] Lee, K., McCormick, W., Ouyang, Q., and Swinney, H.L., *Science* THIS ISSUE
- [2] Selkov, E.E., *Eur. J. Biochem.* **4**, 79 (1968).
- [3] Gray, P. and Scott, S.K., *Chem. Eng. Sci.* **38** 29 (1983); **39**, 1087 (1984); *J. Phys. Chem.* **89** 22 (1985).
- [4] Vastano, J.A., Pearson, J.E., Horsthemke, W., and Swinney, H.L., *Physics Letters A*, **124**, 6,7 320 (1987).
- [5] Segel, L.A., *J. Fluid Mech.* **38** 203 (1969).
- [6] Newell, A.C., Passot, T., and Lega, J., *Annu. Rev. Fluid Mech.*, **25** 399 (1993).
- [7] In this foot–note I describe briefly what is meant by the terms saddle–node and Hopf bifurcations. Consider the ordinary differential equation $d\vec{U}/dt = \vec{F}(\vec{U}; \mu)$ where μ is a control parameter. A saddle–node bifurcation occurs when the number of distinct

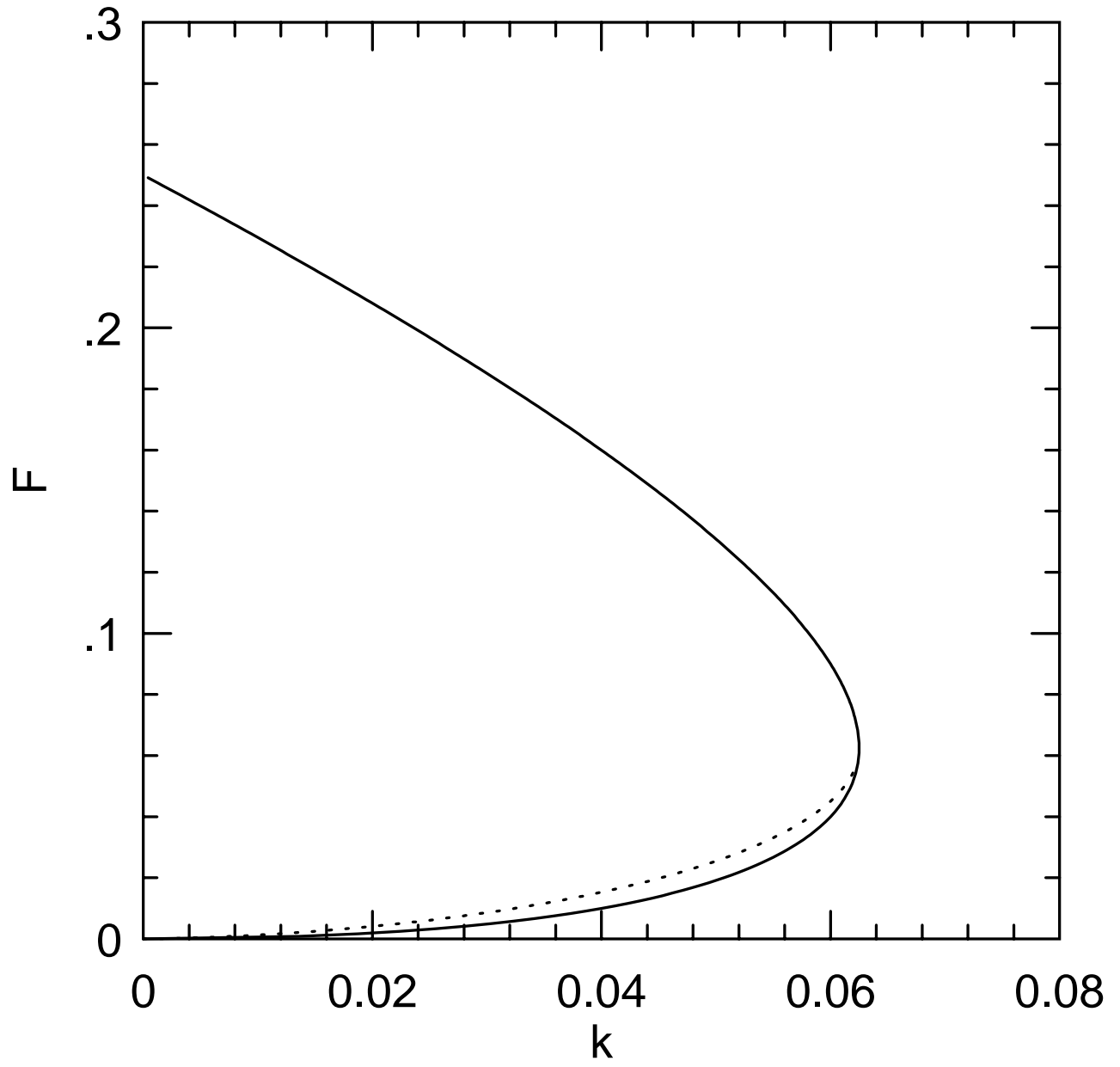
real zeroes of \vec{F} changes as μ is varied. A Hopf bifurcation occurs when the system becomes linearly unstable to oscillatory modes. When a system undergoes a saddle–node bifurcation it settles at a new state which is far from the old state. At a Hopf bifurcation, a branch of periodic solutions appears. This branch may be either stable or unstable.

- [8] J.E. Pearson and W. Horsthemke *J. Chem. Phys.* **90**, 1588 (1989).
- [9] Y. Kuramoto, *Chemical Oscillations, Waves, and Turbulence* Springer–Verlag, 1984
- [10] Pearson, J.E. and Bruno, W. J., *CHAOS*, **2**, 4, 513(1992).
- [11] Vastano, J.A., Pearson, J.E., Horsthemke, W., and Swinney, H.L., *J. Chem. Phys.* **88** (10), 6175 (1988).
- [12] Pearson, J.E., unpublished note
- [13] Hasslacher, B., Kapral, R., and Lawniczak, A., *CHAOS*, **3** 1 (1993).
- [14] I am happy to acknowledge useful conversations with K. Lee, H. Swinney, W. Horsthemke, J. Theiler, S. Ponce–Dawson, and L. Segel. I also thank the Los Alamos Advanced Computing Laboratory for the use of the Connection Machine and A. Chapman, C. Hansen, and P. Hinker for their ever–cheerful assistance with the figures.

Figure Captions

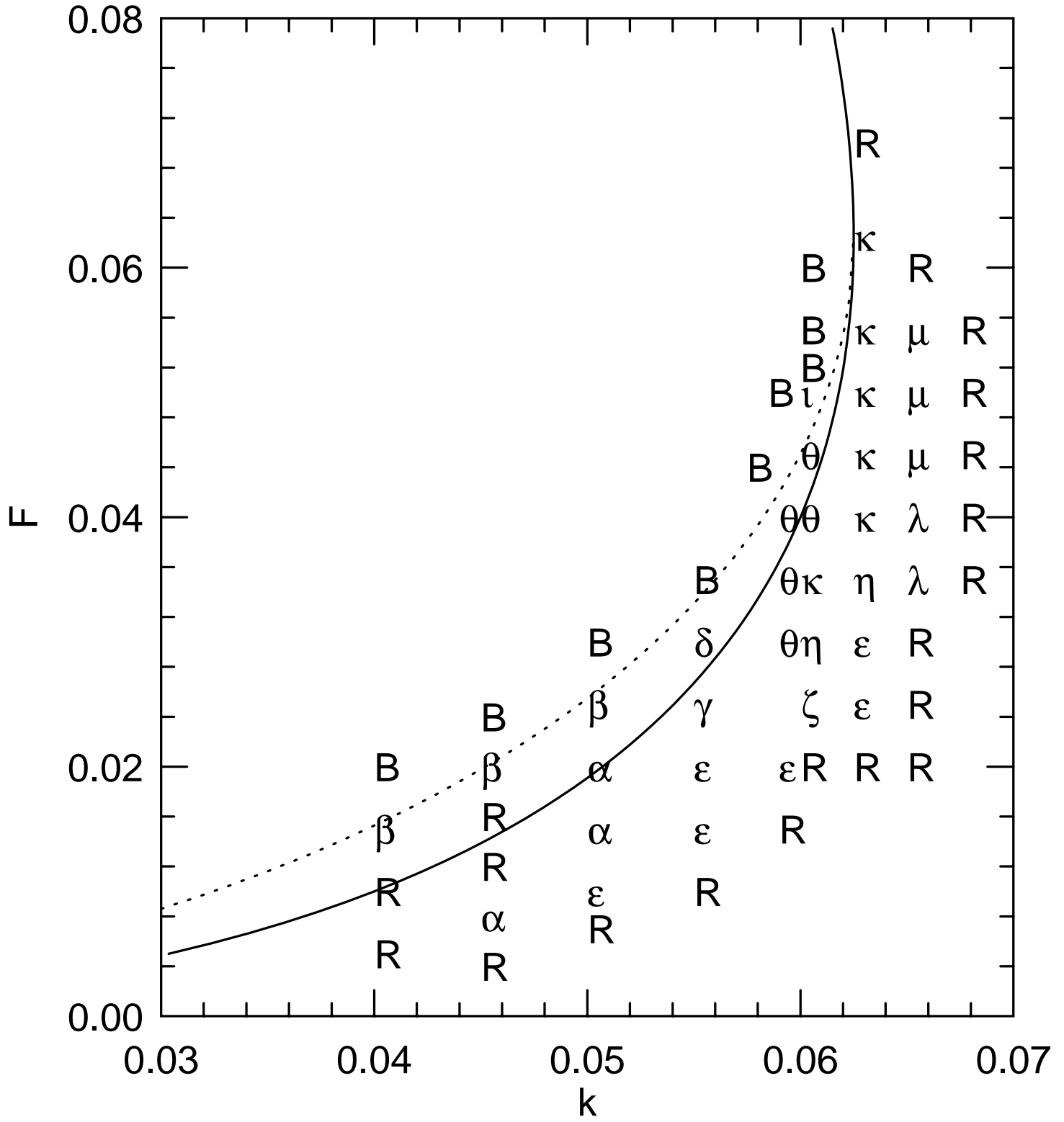
- Figure 1: Phase diagram of the reaction kinetics: Outside the region bounded by the solid line, there is a single spatially uniform state (called the trivial state) ($U = 1, V = 0$) that is stable for all (F, k) . Inside the region bounded by the solid line, there are three spatially uniform steady states. Above the dotted line and below the solid line, the system is bistable: there are two linearly stable steady states in this region. As F is decreased through the dotted line the nontrivial stable steady state loses stability via Hopf bifurcation. The bifurcating periodic orbit is stable for $k < .035$ and unstable for $k > .035$. No periodic orbit exists for parameter values outside the region bounded by the solid line.
- Figure 2: The key to the map. The patterns shown in the figure are designated by Greek letters which are used in Figure 3 to indicate the type of pattern found at a given point in parameter space.
- Figure 3: The map. The Greek letters indicate that a pattern similar to the pattern with the same Greek letter in Figure 2 was found at that point in parameter space. The “B”’s indicate that the system evolved to a uniform blue state. The “R”’s indicate that the system evolved to a uniform red state.
- Figure 4: Time evolution of spot multiplication. This figure was produced in a 256×256 simulation with physical dimensions of $.5 \times .5$ and a time step of $.01$. The times at which the figures were taken is as follows: (A) $T = 0$, (B) $T = 350$, (C) $T = 510$, (D) $T = 650$.
- Figure 5: Time evolution of pattern ε . The images are 250 time units apart. In the corners (which map to the same point in physical space) one can see a yellow region in Figures A-C. It has decayed to red in Figure D. In Figures A-B the center of the left border has a red region which is nearly filled in Figure D.

- Figure 6: Log_{10} -linear plot of D vs t . The center line is the average and the upper and lower lines are the average plus and minus the standard deviation. The straight line has a slope corresponding to a positive Liapunov exponent of about 1.5×10^{-3} .



This figure "fig2.jpg" is available in "jpg" format from:

<http://arxiv.org/ps/patt-sol/9304003v1>



This figure "fig4.jpg" is available in "jpg" format from:

<http://arxiv.org/ps/patt-sol/9304003v1>

This figure "fig5.jpg" is available in "jpg" format from:

<http://arxiv.org/ps/patt-sol/9304003v1>

